Indian Journal of Biochemistry & Biophysics
Vol. 63, September 2026, pp. 1086-1098
DOI: 10.56042/ijbb.v63i9.32338

Integrated GC-MS phytochemical profiling, network pharmacology, and molecular docking to elucidate the molecular mechanisms of *Nymphoides hydrophyllum* against Helminthiasis

Afsona Khatun[1], Nabanita Banik[2], Somali Gorai[2], Ankan Pradhan[2], Monika Sekar[1], Sujay Chakraborty[2] & Thirumal Margesan[1]*

[1]Department of Pharmacognosy, SRM College of Pharmacy, Faculty of Medicine and Health Sciences, SRM Institute of Science and Technology, Kattankulathur, Chengalpattu-603 203, Tamil Nadu, India

[2]Bengal College of Pharmaceutical Technology, Dubrajpur, Birbhum-731 123, West Bengal, India

Received 05 June 2026; *revised 23 July 2026*

Helminthiasis continues to pose a significant worldwide health concern due to the rising resistance to traditional anthelmintic medications and the scarcity of viable treatments. This study sought to provide a scientific foundation for the anthelmintic efficacy of *Nymphoides hydrophyllum* using integrated GC–MS phytochemical profiling, network pharmacology, and molecular docking. GC–MS analysis identified numerous phytoconstituents, with phytol, squalene, and stigmasterol selected for additional computational analysis due to their pharmacological significance and drug-likeness. Network pharmacology research revealed several therapeutic targets linked to kinase-mediated signalling, oxidative stress management, immunological modulation, and cellular survival pathways. GO enrichment analysis revealed substantial participation in protein phosphorylation, membrane-associated signalling, and kinase activity. KEGG pathway enrichment demonstrated a substantial correlation with ErbB signalling, EGFR tyrosine kinase inhibitors resistance, the PD-L1/PD-1 checkpoint pathway, Th17 cell differentiation, PI3K–Akt signalling, and HIF-1 signalling pathways. Numerous hub genes, including EGFR, AKT1, MAPK1, MAPK8, JAK1, JAK2, MTOR, PIK3CA, SRC, and PRKCA, were recognised as pivotal regulators within the pathway-target network. Molecular docking studies revealed advantageous binding relationships between the chosen phytocompounds and target proteins, such as EGFR (5F19), AKT1 (2ITY), MAPK1 (2Y9Q), JAK kinase (5IKR), and acetylcholinesterase (4EJN). Among the evaluated compounds, stigmasterol demonstrated the highest binding affinity for EGFR and acetylcholinesterase, while phytol showed a favourable interaction with JAK kinase and Squalene demonstrated moderate binding affinity with acetylcholinesterase. The findings indicate that *N. hydrophyllum* exhibits significant anthelmintic potential by modulating many signalling pathways and parasite-related cellular mechanisms.

Keywords: Anthelmintic efficacy, Oxidative stress, Immunological modulation, Signalling pathways

Medicinal plants have been crucial to therapeutic practices across various cultures for centuries, providing a wealth of bioactive compounds for the treatment of numerous diseases and ailments[1]. The genus Nymphoides, comprising around 50 species worldwide, is of considerable ethnomedicinal importance owing to its diverse biological traits and therapeutic uses. Different parts of plants, including stalks, leaves, and seeds, have historically been utilized in the management of a wide range of health issues, including jaundice, fever, and skin infections[2]. Ethnobotanical surveys provide additional evidence for the widespread application of Nymphoides species within traditional medicinal practices, particularly for the treatment of ailments such as dysentery, pyrexia, scabies, convulsions, and various systemic disorders[3]. The records of these practices are extensive across various regions, notably in India, Thailand, and Nepal, where local formulations from this genus continue to play a crucial role in community-based healthcare strategies[3–5].

Nymphoides hydrophyllum is a free-floating aquatic herb belonging to the family Menyanthaceae, found in freshwater ecosystems across India, Bangladesh, Bhutan, and Cambodia. This species is notable for its unique morphology, with orbicular-cordate leaves measuring 8–10 cm in breadth. The leaves exhibit a purplish coloration with prominent green venation and are accompanied by densely fasciculated white corollas at the stem nodes[6,7]. It is also a rare aquatic vegetable, a delicacy of the Hakka people in Taiwan[8]. The leaves have been found to contain six essential amino acids, in addition to a

*Correspondence:
E-mail: thirumam@srmist.edu.in

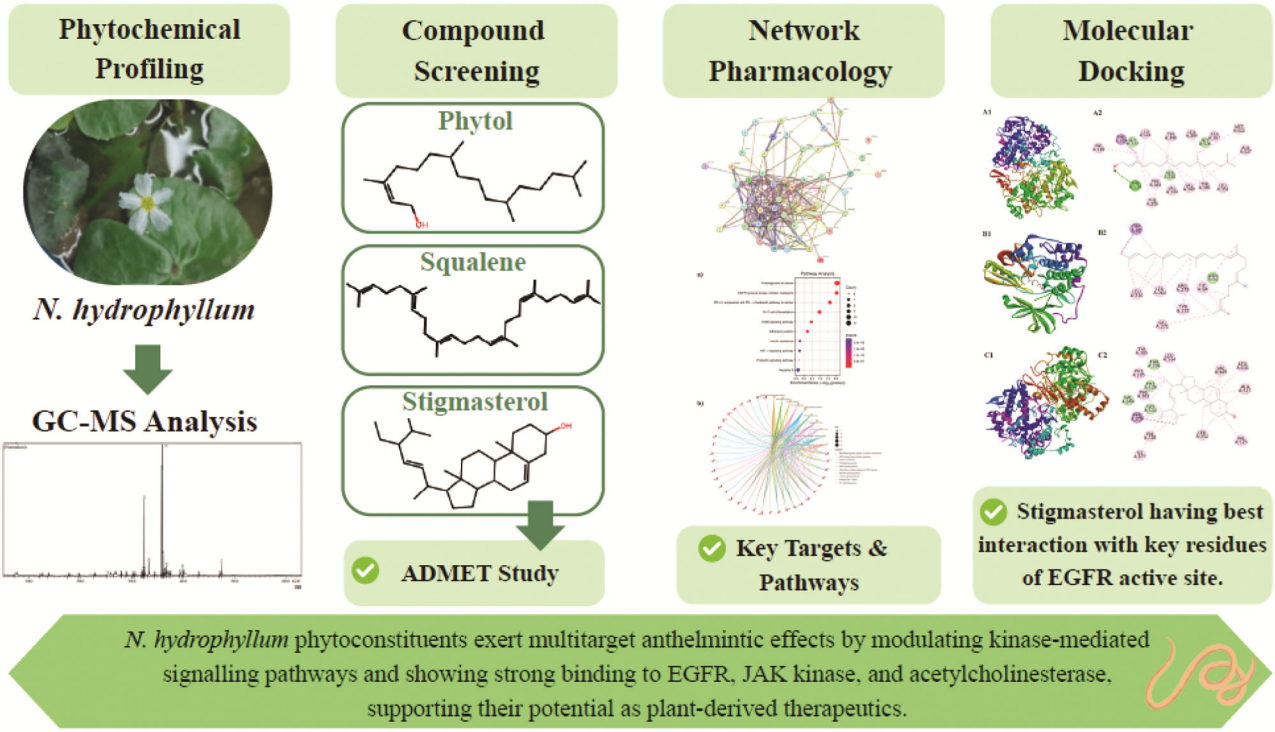

Graphical abstract

notable protein content, highlighting their nutritional and potential pharmacological significance[6]. While generally exhibiting an annual growth pattern, it may also exhibit perennial traits under favourable environmental conditions.

Helminthiasis, a parasitic infection caused by helminths, continues to pose a significant public health challenge, especially in developing nations where socioeconomic constraints hinder access to adequate healthcare[9]. Despite the presence of synthetic anthelmintic agents, challenges, including the emergence of drug resistance, host toxicity, and the intricate antigenic characteristics of parasites, which hinder vaccine development, have heightened the pursuit of alternative therapeutic strategies[2]. In this context, medicinal plants offer a significant opportunity to identify new anthelmintic compounds that are both effective and safe while remaining sustainable.

Therefore, this work aims to establish a comprehensive scientific basis for the anti-helminthiasis property of *N. hydrophyllum*. This study employs various analytical techniques, including phytochemical screening, network pharmacology to elucidate compound-target-pathway interactions, and molecular docking to predict binding affinities between bioactive compounds and critical parasitic targets. This multi-omics approach seeks to clarify the mechanistic basis of the antihelminthiasis property of *N. hydrophyllum*, thereby aiding the rational development of plant-based treatments for helminthiasis.

Materials and Methods

Collection of plant material

Plant material was collected from muddy pond water from the rural area of Dubrajpur, Birbhum, West Bengal, India. In the voucher no CNH/Tech.III/2025/129 identification was carried out at the Botanical Survey of India, Central National Herbarium, Howrah 711316, West Bengal, India.

Preparation of extract

The whole plant was collected and pulverised into powder using a mixer grinder. The powder weighing about 5 gm was transferred into the beaker. The sample was macerated separately in ethanol and chloroform for about 7 days in a well-closed container. The two extracts were poured out, and another consecutive maceration was followed again with ethanol for the next 7 days. The filtered extracts were collected in a closed container. Both extracts (50 mL each) were poured into a 100 ml beaker and allowed to evaporate at room temperature to obtain

concentrated extracts. 10 ml of each concentrated extract was used for GC-MS investigation. None of the heating methods was used in the entire extraction process. This was done to avoid degrading thermolabile compounds[10].

GC-MS phytochemical profiling

Extracts were analysed using a Shimadzu QP 2010 Ultra GC-MS at the central instrumentation laboratory of the Central University of Punjab in Ghudda, Bathinda, to detect volatile bioactive phytoconstituents. The chromatographic separation was performed according to compound retention time, followed by mass spectral detection using an electron ionisation (EI) mass analyser. The discovered substances were identified by comparing their fragmentation patterns and retention indices with those catalogued in the NIST Mass Spectral Library[11]. The principal chemicals were identified with retention times between roughly 36.4 and 37.7 min.

ADMET screening

The phytoconstituents detected by GC-MS analysis of N. hydrophyllum were initially evaluated using their chromatographic peak-area percentages. Compounds with peak areas of less than 1% were excluded to minimise the inclusion of trace elements with low abundance and limited pharmacological significance. The remaining significant phytoconstituents were chosen for subsequent pharmacokinetic and toxicological assessment. The canonical SMILES of the discovered compounds were obtained from PubChem and examined using the SwissADME and Protox-II 3.0 software[12,13]. Parameters such as gastrointestinal absorption, Lipinski's rule of five, bioavailability score, and projected toxicity class were assessed. Compounds demonstrating advantageous pharmacokinetic characteristics, acceptable toxicity levels, and significant biological significance were chosen for further network pharmacology and molecular docking analyses.

Target prediction and disease target collection

The chosen compounds demonstrating advantageous ADMET properties underwent target prediction analysis utilizing the online prediction platform SwissTargetPrediction[14]. The canonical SMILES of the compounds served as the input, with Homo sapiens designated as the target organism.

A thorough investigation was conducted to gather disease-associated targets pertinent to helminthiasis and anthelmintic activity, using comprehensive database mining techniques with resources such as GeneCards, and DisGeNET[15,16]. The search process utilized terms such as “anthelmintic,” “helminth infection,” “parasitic infection,” and “helminthiasis.” The disease-related targets identified were meticulously curated, with duplicate genes systematically excluded from the dataset.

The intersection of predicted compound-associated targets and disease-associated targets was performed using a Venn diagram generated with Venny 2.1.0 to identify common therapeutic targets.

Protein–protein interaction (PPI) network construction

PPI networks were constructed to explore functional relationships among overlapping targets associated with the anticipated anthelmintic properties of *N. hydrophyllum*. The identification of interacting proteins is crucial for elucidating the intricate molecular mechanisms that govern biological responses, signal transduction, neuromuscular regulation, and the survival pathways of parasites linked to helminth infections. The targets identified from the overlap of phytoconstituent-associated targets and helminthiasis-related targets were subsequently imported into the STRING database to construct the PPI network, with the analysis restricted to Homo sapiens[17]. An elevated threshold for interaction-score confidence was implemented to mitigate false-positive interactions and enhance the network's reliability. The generated network was subsequently exported and visualized in Cytoscape version 3.10.4[18].

Pathway enrichment analysis

Gene Ontology (GO) functional annotation and Kyoto Encyclopedia of Genes and Genomes (KEGG) pathway enrichment analyses were conducted to assess the biological significance and functional roles of overlapping targets associated with the anticipated anthelmintic activity of *N. hydrophyllum*. The therapeutic targets identified using Venn analysis were submitted to ShinyGO 0.85.1 for enrichment analysis[19]. Statistically significant routes were determined using false discovery rate (FDR) values and enrichment scores. The priority routes for further interpretation include those related to neurotransmission, inflammatory signalling, signal transduction, oxidative stress, and processes of parasite persistence. The most enriched KEGG pathways were illustrated using bubble plots and bar graphs created with SRplot to

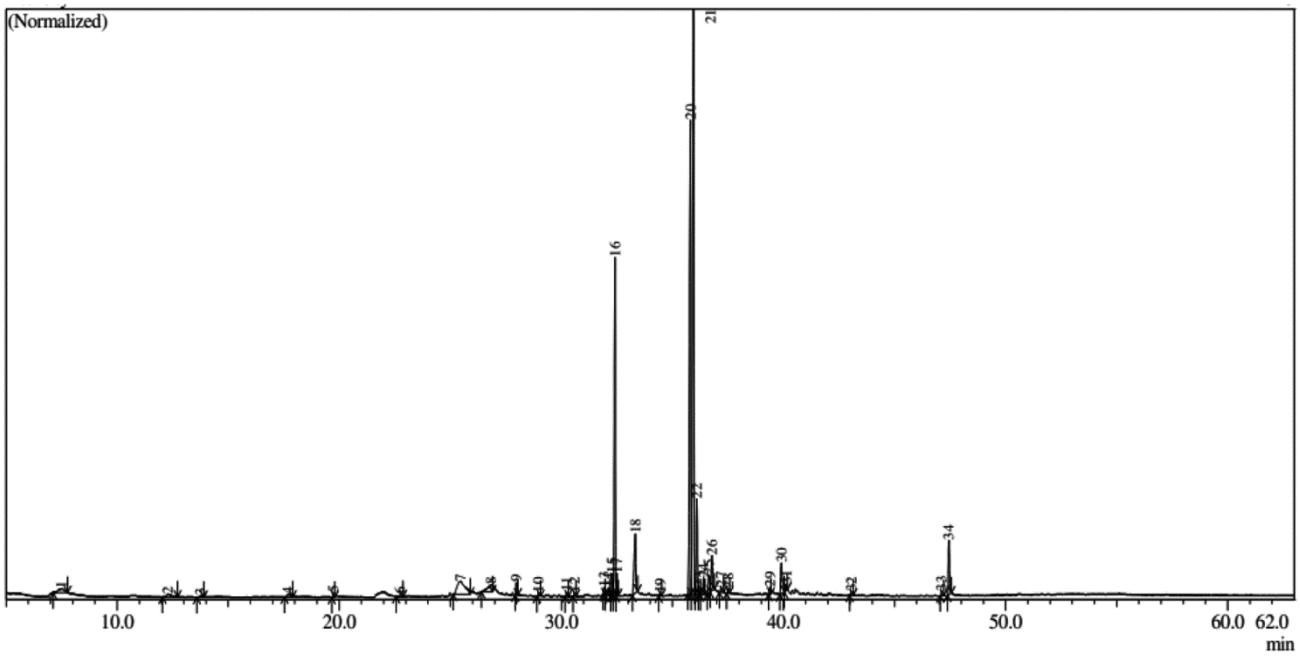

Fig. 1 — GC-MS chromatogram of the ethanolic extract of *N. Hydrophyllum*

enable comparative route analysis and visual representation[20].

Molecular docking

Molecular docking study was conducted to assess the binding interactions between potent compounds from *N. hydrophyllum* and selected target proteins associated with helminthiasis. The three-dimensional crystal structures of the target proteins were obtained from the Protein Data Bank in PDB format[21]. Protein structures were constructed with AutoDock Tools by eliminating water molecules, co-crystallized ligands, and other heteroatoms, subsequently including polar hydrogen atoms and Kollman charges. The protein structures were subsequently stored in PDBQT format. Then, the chemical structures of the chosen phytocompounds were acquired from PubChem in SDF format and subsequently translated to PDB format with Open Babel[22,23]. Prior to docking, the optimised ligand structures were saved in PDBQT format.

Molecular docking was conducted via AutoDock 1.5.7. The grid box dimensions were modified to encompass the active binding site region of each target protein. The Lamarckian genetic method was utilised to predict the best binding conformations and to compute binding affinity values in kcal/mol. The docked complexes exhibiting the lowest binding energy and advantageous interaction patterns were chosen for subsequent study.

The molecular interactions, such as hydrogen bonding, hydrophobic interactions, π–π stacking, and van der Waals forces, between ligands and target proteins were examined and visualised using Discovery Studio Visualiser. The docking data were analysed to elucidate the potential molecular pathways underlying the mechanism of action of *N. hydrophyllum* phytoconstituents against Helminthiasis.

Results and Discussion

GC–MS phytochemical profiling

The GC-MS chromatogram of the ethanolic extract of *N. hydrophyllum* revealed 34 peaks (Fig. 1), and the chloroform extract revealed 26 peaks (Fig. 2), indicating the presence of 34 and 26 phytochemical components. Total phytocompounds identified from the ethanolic extract are listed in (Table 1), and those from the chloroform extract are listed in (Table 2).

Compound screening and target prediction

Although a total of 60 compounds were detected by GC-MS, only 25 exceeded 1% of the area in the initial screening. Following the ADMET analysis (Table 3), a total of 3 compounds (Phytol, Squalene and Stigmasterol) were identified for selection, based on their pharmacokinetic properties, acceptable toxicity-profiles, and notable biological relevance.

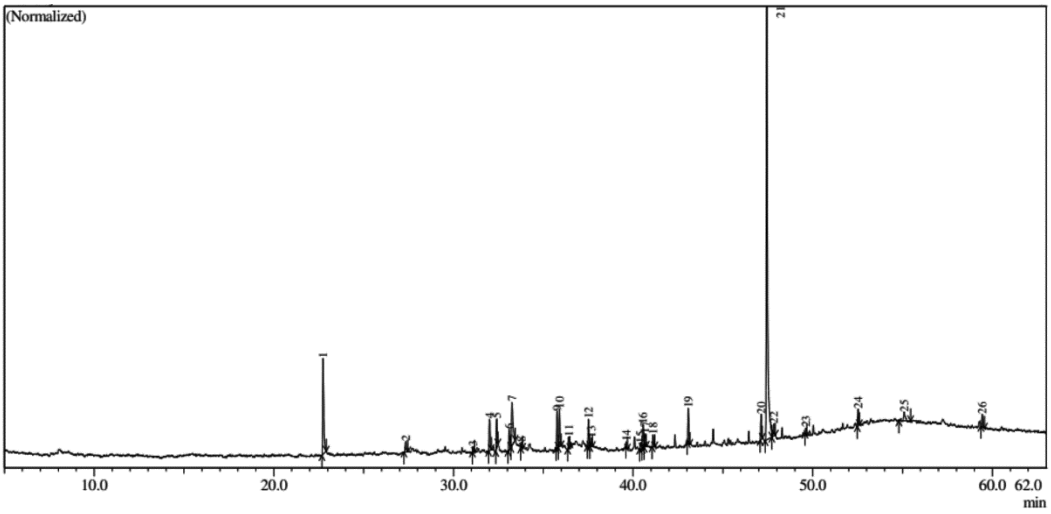

Fig. 2 — GC-MS chromatogram of the chloroform extract of *N. hydrophyllum*

Table 1 — GC-MS analysis of phytocomponents from the ethanolic extract of *N. hydrophyllum*

Peak	R. Time	Area %	Name	Formula	MW
1	7.470	0.94	Glycerin	$C_3H_8O_3$	92
2	12.274	0.54	4H-Pyran-4-one	$C_6H_8O_4$	144
3	13.753	0.18	Dodecane	$C_{12}H_{26}$	170
4	17.687	0.41	beta-D-Ribopyranoside, methyl	$C_6H_{12}O_5$	164
5	19.744	0.19	Tetradecane	$C_{14}H_{30}$	198
6	22.743	0.12	Phenol, 3,5-bis(1,1-dimethylethyl)-	$C_{14}H_{22}O$	206
7	25.453	4.22	alpha-D-Glucopyranoside, methyl	$C_7H_{14}O_6$	194
8	26.835	1.56	2-Deoxy-D-galactose	$C_6H_{12}O_5$	164
9	27.973	0.47	Methyl tetradecanoate	$C_{15}H_{30}O_2$	242
10	28.964	0.19	Pentadecanoic acid	$C_{15}H_{30}O_2$	242
11	30.232	0.16	Pentadecanoic acid, methyl ester	$C_{16}H_{32}O_2$	256
12	30.600	0.13	2-Pentadecanone, 6,10,14-trimethyl-	$C_{18}H_{36}O$	268
13	31.925	0.25	9-Hexadecenoic acid, methyl ester, (Z)-	$C_{17}H_{32}O_2$	268
14	32.135	0.40	(Z)-Methyl hexadec-11-enoate	$C_{17}H_{32}O_2$	268
15	32.277	0.85	7-Hexadecenoic acid, methyl ester, (Z)-	$C_{17}H_{32}O_2$	268
16	32.412	13.85	Hexadecanoic acid, methyl ester	$C_{17}H_{34}O_2$	270
17	32.491	0.86	Benzenepropanoic acid, 3,5-bis (1,1-dimethylethyl)-4-hydroxy	$C_{18}H_{28}O_3$	292
18	33.326	3.86	n-Hexadecanoic acid	$C_{16}H_{32}O_2$	256
19	34.438	0.12	Heptadecanoic acid, methyl ester	$C_{18}H_{36}O_2$	284
20	35.806	24.25	9,12-Octadecadienoic acid (Z,Z)-, methyl ester	$C_{19}H_{34}O_2$	294
21	35.951	32.26	9,12,15-Octadecatrienoic acid, methyl ester	$C_{19}H_{32}O_2$	292
22	36.099	4.02	Phytol	$C_{20}H_{40}O$	296
23	36.217	0.33	trans-13-Octadecenoic acid, methyl ester	$C_{19}H_{36}O_2$	296
24	36.403	0.66	Methyl stearate	$C_{19}H_{38}O_2$	298
25	36.640	1.12	9,12-Octadecadienoic acid (Z,Z)-	$C_{18}H_{32}O_2$	280
26	36.780	2.06	9,12,15-Octadecatrienoic acid, (Z,Z,Z)-	$C_{18}H_{30}O_2$	278
27	37.180	0.26	Octadecanoic acid	$C_{18}H_{36}O_2$	284
28	37.510	0.18	Hexadecanoic acid, butyl ester	$C_{20}H_{40}O_2$	312
29	39.394	0.36	4,8-Decadienal, 5,9-dimethyl-	$C_{12}H_{20}O$	180
30	39.901	1.98	Isopropyl phenyl ketone	$C_{10}H_{12}O$	148
31	40.125	0.35	Tricyclo[20.8.0.0(7,16)] triacontane, 1(22),7(16)-diepoxy-	$C_{30}H_{52}O_2$	444
32	43.059	0.15	13-Docosenoic acid, methyl ester, (Z)-	$C_{23}H_{44}O_2$	352
33	47.123	0.20	22-Tricosenoic acid	$C_{23}H_{44}O_2$	352
34	47.447	2.52	13-Docosenamide, (Z)-	$C_{22}H_{43}NO$	337

Table 2 — GC-MS analysis of phytocomponents from the chloroform extract of *N. hydrophyllum*

Peak	R. Time	Area %	Name	Formula	MW
1	22.744	9.45	Phenol, 3,5-bis(1,1-dimethylethyl)-	$C_{14}H_{22}O$	206
2	27.347	1.37	Hexadecyl acrylate	$C_{19}H_{36}O_2$	296
3	31.091	0.52	1,2-Benzenedicarboxylic acid, bis(2-methylpropyl) ester	$C_{16}H_{22}O_4$	278
4	32.011	2.72	7,9-Di-tert-butyl-1-oxaspiro (4,5) deca-6,9-diene-2,8-dione	$C_{17}H_{24}O_3$	276
5	32.409	2.22	Hexadecanoic acid, methyl ester	$C_{17}H_{34}O_2$	270
6	33.102	2.08	Dibutyl phthalate	$C_{16}H_{22}O4$	278
7	33.259	6.16	n-Hexadecanoic acid	$C_{16}H_{32}O_2$	256
8	33.788	0.43	1-Tricosene	$C_{23}H_{46}$	322
9	35.77	2.9	9,11-Octadecadienoic acid, methyl ester	$C_{19}H_{34}O_2$	294
10	35.898	3.3	8,11,14-Docosatrienoic acid, methyl ester	$C_{23}H_{40}O_2$	348
11	36.415	0.94	Methyl stearate	$C_{19}H_{38}O_2$	298
12	37.518	2.12	Hexadecanoic acid, butyl ester	$C_{20}H_{40}O_2$	312
13	37.677	0.83	4-Tetradecanol	$C_{14}H_{30}O$	214
14	39.622	0.33	9-Hexadecenoic acid, methyl ester, (Z)-	$C_{17}H_{32}O_2$	268
15	40.408	0.59	6,6-Dibutoxyhexanoic acid, butyl ester	$C_{18}H_{36}O_4$	316
16	40.56	2.36	2H-Benzocyclohepten-2-one, decahydro-4a-methyl-	$C_{12}H_{20}O$	180
17	40.642	1.46	7-Tetradecenal, (Z)-	$C_{14}H_{26}O$	210
18	41.105	1.01	Octadecanoic acid, butyl ester	$C_{22}H_{44}O_2$	340
19	43.07	2.7	13-Docosenoic acid, methyl ester, (Z)-	$C_{23}H_{44}O_2$	352
20	47.13	1.83	Erucic acid	$C_{22}H_{42}O_2$	338
21	47.446	48.78	13-Docosenamide, (Z)-	$C_{22}H_{43}NO$	337
22	47.835	1.32	Squalene	$C_{30}H_{50}$	410
23	49.614	0.47	trans-2-Hexadecenoic acid	$C_{16}H_{30}O_2$	254
24	52.529	1.27	4-(5-Bromo-3-tert-butylsalicyl)-2,6-di-tert-butylphenol	$C_{25}H_{35}BrO_2$	446
25	55.09	1.4	Stigmasterol	$C_{29}H_{48}O$	412
26	59.434	1.45	Tris(2,4-di-tert-butylphenyl) phosphate	$C_{42}H_{63}O_4P$	662

Table 3 — ADMET Screening of selected compounds from the ethanolic and chloroform extract of *N. hydrophyllum*

PubChem ID	Compound Name	BS	GIA	LV	CT	LD_{50}
5280450	9,12-Octadecadienoic acid (Z,Z)-	0.85	High	1	Low	10000 mg/kg
102191	2-Deoxy-D-galactose	0.55	Low	0	Low	20000 mg/kg
69144	Isopropyl phenyl ketone	0.55	High	0	Low	3000 mg/kg
5365371	13-Docosenamide, (Z)-	0.55	Low	1	Moderate	750 mg/kg
985	n-Hexadecanoic acid	0.85	High	1	Moderate	900 mg/kg
5280435	Phytol	0.55	Low	1	Low	5000 mg/kg
64947	alpha-D-Glucopyranoside, methyl	0.55	Low	0	Low	23000 mg/kg
8181	Hexadecanoic acid, methyl ester	0.55	High	1	Low	5000mg/kg
5284421	9,12-Octadecadienoic acid (Z,Z)-, methyl ester	0.55	High	1	Low	20000 mg/kg
5367462	9,12,15-Octadecatrienoic acid, methyl ester	0.55	High	1	Low	20000 mg/kg
31278	Octadecanoic acid, butyl ester	0.55	Low	1	Low	5000 mg/kg
545465	4-(5-Bromo-3-tert-butylsalicyl)-2,6-di-tert -butylphenol	0.55	Low	1	Low	3430 mg/kg
638072	Squalene	0.55	Low	1	Low	5000 mg/kg
83410	hexadecyl acrylate	0.55	High	1	Low	5000 mg/kg
5280794	Stigmasterol	0.55	Low	1	Moderate	890 mg/kg
14572930	Tris(2,4-di-tert-butylphenyl) phosphate	0.55	Low	2	Low	15800 mg/kg
5364468	7-Tetradecenal, (Z)-	0.55	High	0	Low	5000 mg/kg
5281116	Erucic acid	0.85	Low	1	High	48 mg/kg

(*Contd.*)

Table 3 — ADMET Screening of selected compounds from the ethanolic and chloroform extract of *N. hydrophyllum.* (*Contd.*)

PubChem ID	Compound Name	BS	GIA	LV	CT	LD_{50}
8090	Hexadecanoic acid, butyl ester	0.55	Low	1	Low	5000 mg/kg
	2H-Benzocyclohepten-2-one, decahydro-9a-methyl-	0.55	High	0	Low	2400 mg/kg
5364423	13-Docosenoic acid, methyl ester, (Z)-	0.55	Low	1	Low	3000 mg/kg
545303	7,9-Di-tert-butyl-1-oxaspiro (4,5) deca-6,9-diene-2,8-dione	0.55	High	0	Moderate	900 mg/kg
5365686	9,11-Octadecadienoic acid, methyl ester	0.55	High	1	Low	5000 mg/kg
5364473	8,11,14-Docosatrienoic acid, methyl ester	0.55	Low	1	Low	20000 mg/kg
70825	Phenol, 3,5-bis(1,1-dimethylethyl)-	0.55	High	0	Moderate	800 mg/kg

BS, bioavailability score; GIA, gastrointestinal absorption; LV, number of Lipinski's rule of five violations; CT, class of toxicity

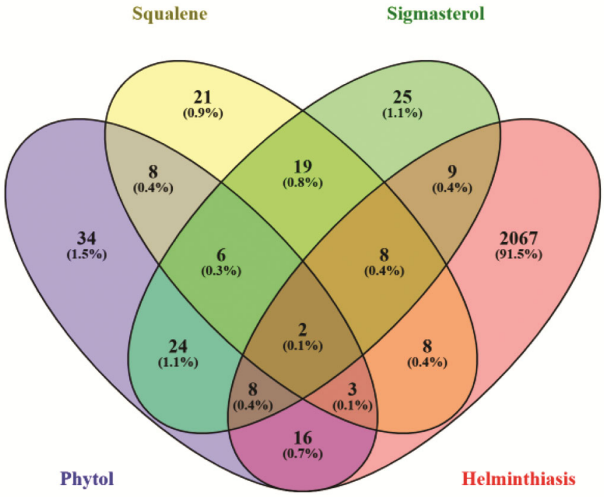

Fig. 3 — Venn diagram of Phytol, Squalene and Stigmasterol with target proteins of Helminthiasis

After removing duplicates, 2,251 proteins associated with target genes relevant to helminthic infection were identified in the GeneCards and DisGeNET databases. Later, for all three compounds, a total of 189 target genes is predicted by the SwissTargetPrediction tool. Finally, a total of 54 common genes are identified by the Venn diagram (Fig. 3).

Protein–protein interaction (PPI) network analysis

The PPI network was constructed by importing the selected target genes into the STRING online database. Figure 4 shows the final network topology, which included 54 proteins (nodes) and 239 interactions (edges). Cytoscape was used to import the network for topological analysis, enabling further visualization and investigation of protein interaction patterns. A significant degree of connection among the proteins was indicated by the network's average node degree of 8.81. Also, the network appears to have strongly related functional modules, as indicated by an average local clustering coefficient of 0.485.

The observed number of edges (239) was far higher than the expected number of edges (94), suggesting that the proteins were much more interconnected than would be expected from a random calculation alone (Table 4). The statistical significance and biological importance of the interaction network were confirmed by a PPI enrichment p-value of less than 1.0×10^{-16}. These results indicate that the identified targets are involved in coordinated biological processes and signalling pathways related to disease progression.

Analysis of KEGG pathways and GO function enrichment

The GO enrichment analysis indicated that the identified targets were significantly enriched for various biological processes (BP), cellular components (CC), and molecular functions (MF) (Fig. 5). The principal enriched phrases in the BP category comprised peptidyl-tyrosine phosphorylation, peptidyl-tyrosine modification, positive modulation of protein transport, positive regulation of establishment of protein localization, regulation of body fluid levels, peptidyl-serine phosphorylation, histone phosphorylation, positive regulation of cytosolic calcium ion concentration, phosphatidylinositol-mediated signalling, and wound healing. The results suggest that the active phytoconstituents of *N. hydrophyllum* may modulate intracellular signalling, phosphorylation-mediated processes, calcium homeostasis, and stress-responsive cellular mechanisms associated with parasite survival. In the CC category, the enriched targets were primarily linked to membrane microdomains, plasma membrane rafts, caveola, endoplasmic reticulum lumen, multivesicular body, late endosome, cytoplasmic side of membrane, endolysosome, and endosome lumen, indicating that the predicted targets are predominantly situated in membrane-associated signalling regions and intracellular transport compartments. The MF analysis revealed substantial enrichment in transmembrane receptor protein tyrosine kinase activity, protein tyrosine kinase activity, non-membrane spanning protein tyrosine

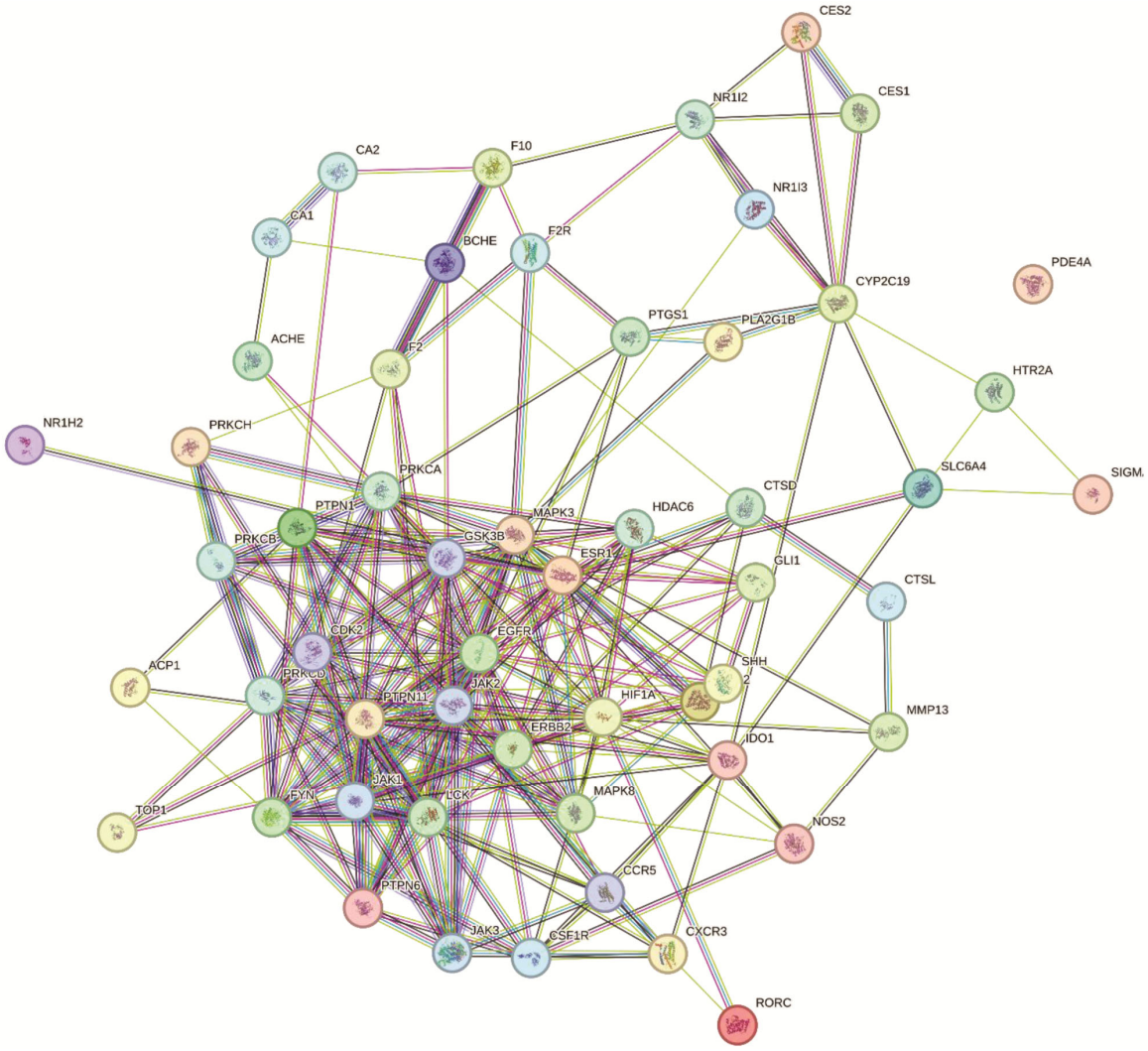

Fig. 4 — PPI Network

Table 4 — PPI network of compounds protein and diseases proteins

Number of nodes	54
Number of edges	239
Average node degree	8.81
Avg. Local clustering coefficient	0.485
Expected number of edges	94
PPI enrichment p-value	< 1.0e-16

tyrosine kinase activity, nuclear receptor activity, ligand-activated transcription factor activity, calcium-dependent protein kinase C activity, histone kinase activity, protein kinase C activity, and protein serine/threonine kinase activity. Kinase-mediated regulatory mechanisms may be essential for the pharmacological effects of *N. hydrophyllum* phytoconstituents.

KEGG pathway enrichment analysis revealed multiple significantly enriched pathways associated with inflammation, cellular survival, and signal transduction (Fig. 6). Among these, EGFR tyrosine kinase inhibitor resistance exhibited the greatest enrichment and target engagement, followed by PD-L1 expression and PD-1 checkpoint pathway in cancer, Prolactin signalling pathway, and ErbB signalling pathway. Additional enriched pathways encompassed the adherens junction, Th17 cell differentiation, HIF-1 signalling pathway, insulin resistance, serotonergic synapse, T cell receptor signalling pathway, chemokine signalling pathway, proteoglycans in cancer, hepatitis B, pathways in cancer, and the PI3K–Akt signalling pathway.

The pathway-target interaction network further illustrated that several hub genes, including EGFR,

Fig. 5 — Bar graph representing Gene Ontology (GO) enrichment analysis results for the three main GO categories: Biological Process (BP), Cellular Component (CC), and Molecular Function (MF). Enrichment was considered significant at a p-value cutoff of 0.05

AKT1, MAPK1, MAPK8, JAK1, JAK2, MTOR, PIK3CA, SRC, and PRKCA, were involved in numerous enriched pathways, indicating their pivotal role in the multitarget therapeutic efficacy of *N. hydrophyllum* phytocompounds. These data collectively suggest that the identified phytochemicals may have anthelmintic action via modulating kinase-related signalling pathways, oxidative stress responses, inflammatory regulation, and parasite-related cellular processes.

Molecular docking

The hub proteins identified through KEGG pathway enrichment analysis were selected for docking experiments, including EGFR (PDB ID: 5F19), AKT1 (PDB ID: 2ITY), MAPK1 (PDB ID: 2Y9Q), JAK kinase (PDB ID: 5IKR), and acetylcholinesterase (PDB ID: 4EJN) (Table 5).

Among the evaluated phytoconstituents, stigmasterol demonstrated the highest binding affinity for EGFR (PDB ID: 5F19) with a docking score of −12.53 kcal/mol, followed by acetylcholinesterase (4EJN) with a binding affinity of −10.99 kcal/mol, signifying persistent ligand–protein interactions. Phytol exhibited advantageous binding with EGFR and JAK kinase, yielding docking scores of −8.38 kcal/mol and −8.69 kcal/mol, respectively. Squalene showed modest affinity for EGFR (−7.16 kcal/mol) and acetylcholinesterase (−7.32 kcal/mol). The best interaction of each compound is given in (Fig. 7).

The docking interactions indicate that EGFR and acetylcholinesterase could be significant molecular targets for the phytoconstituents of *N. hydrophyllum*. The robust interaction between stigmasterol and EGFR suggests its potential role in regulating kinase-mediated signalling pathways identified *via* KEGG enrichment analysis. The combination of phytol and

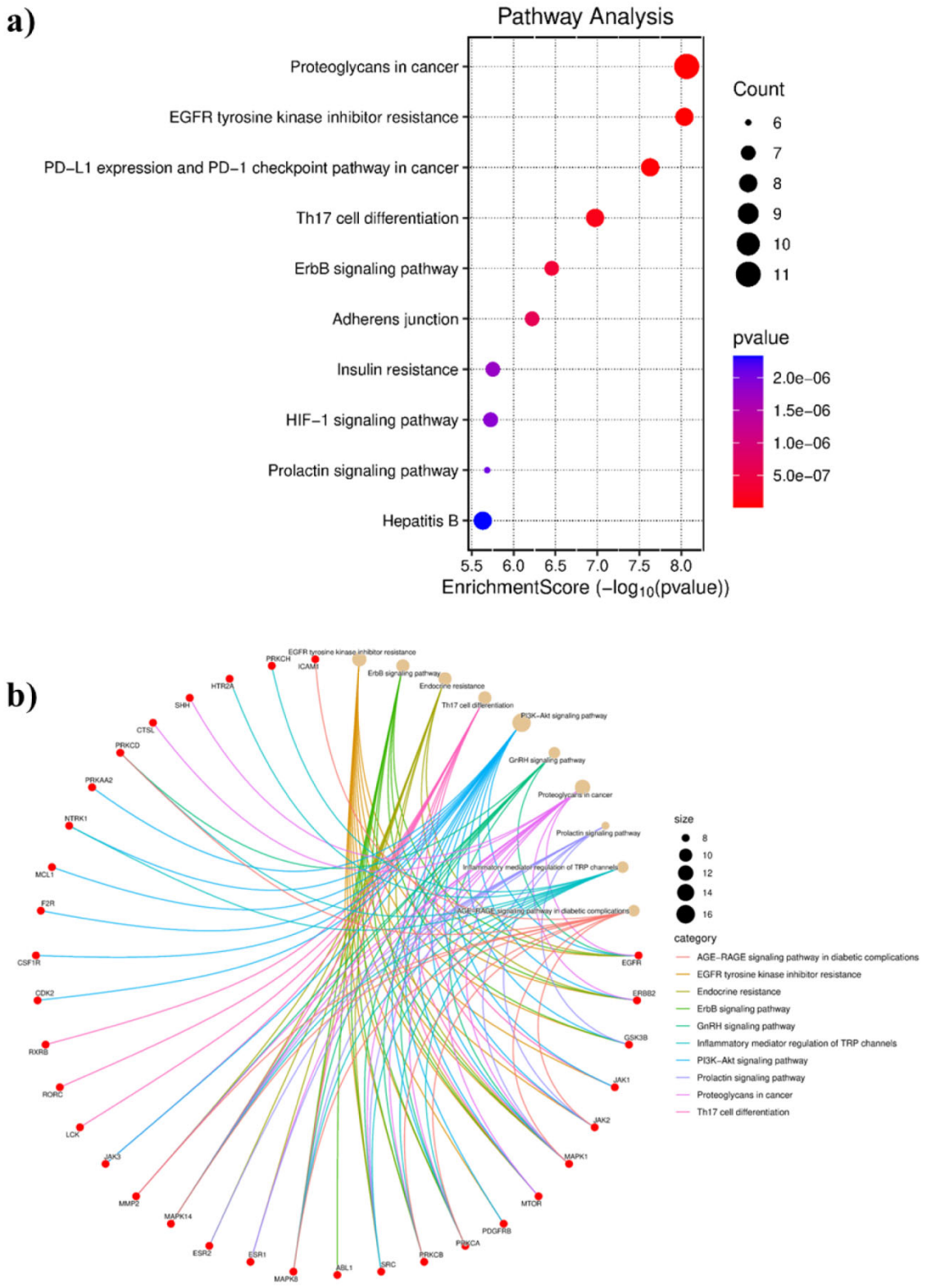

Fig. 6 — (a) KEGG bubble chart showing 10 Pathway Enrichment; and (b) Gene-Pathway Interaction Network: Enriched KEGG Signalling Pathways

Table 5 — List of docking scores (kcal/mol) of Proteins-Ligand dockings

Protein	PDB Id	Attributes	Ligand/compound	Binding affinity (kcal/mol)
EGFR	5F19	X= 20.808138	Phytol	-8.38
		Y= 37.471304	Squalene	-7.16
		Z= 59.330668	Stigmasterol	-12.53
AKT1	2ITY	X= -58.406331	Phytol	17.9
		Y= -7.986654	Squalene	359.3
		Z= -24.505475	Stigmasterol	161.4
MAPK1	2Y9Q	X= 58.805925	Phytol	29.03
		Y= 25.181817	Squalene	186.22
		Z= 6.913085	Stigmasterol	454.5
JAK kinase	5IKR	X= 32.087261	Phytol	-8.69
		Y= 6.608363	Squalene	-6.05
		Z= 58.922840	Stigmasterol	7.22
AChE	4EJN	X= 32.007434	Phytol	-6.28
		Y= 41.180042	Squalene	-7.32
		Z= 13.458169	Stigmasterol	-10.99

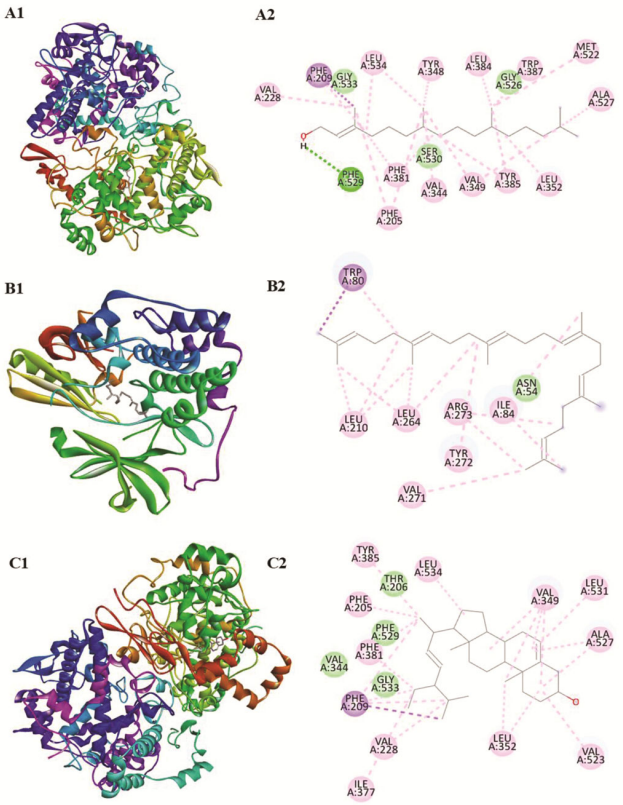

Fig. 7 — Visualizing the molecular docking with Helminthiasis-related targets. A1 and A2 are the 3D and 2D images of Phytol with 5IKR, B1 and B2 are the 3D and 2D images of Squalene with 4EJN, C1 and C2 are the 3D and 2D images of Stigmasterol with 5F19.

stigmasterol with acetylcholinesterase suggests a possible neuromuscular inhibitory mechanism that contributes to anthelmintic activity.

Conclusion

This study provided a thorough scientific foundation for the anthelmintic potential of *N. hydrophyllum* through integrated GC-MS-based phytochemical profiling, network pharmacology, and molecular docking. The GC–MS study identified a total of 60 phytoconstituents. Among them, a total of three compounds, Phytol, Squalene and Stigmasterol are selected based on ADMET and pharmacological relevance.

Network pharmacology analysis revealed that the anticipated targets of the identified phytochemicals were significantly enriched in various biological processes and signalling pathways related to kinase regulation, oxidative stress response, immune modulation, and cellular survival mechanisms. GO enrichment analysis revealed substantial participation in protein phosphorylation, membrane-associated signalling, intracellular transport, and kinase-mediated molecular activities. KEGG pathway enrichment analysis revealed several significant pathways, including resistance to EGFR tyrosine kinase inhibitors, PD-L1/PD-1 checkpoint signalling, Th17 cell differentiation, HIF-1 signalling, PI3K–Akt signalling, ErbB signalling, and chemokine signalling pathways, indicating the multitarget therapeutic potential of *N. hydrophyllum* phytoconstituents.

The pathway target interaction network revealed critical hub genes, including EGFR, AKT1, MAPK1, MAPK8, JAK1, JAK2, MTOR, PIK3CA, SRC, and PRKCA, underscoring their significant involvement in compound target pathway interactions. The molecular docking investigation confirmed the interaction potential

of the chosen phytocompounds with key target proteins, namely EGFR (5F19), AKT1 (2ITY), MAPK1 (2Y9Q), JAK kinase (5IKR), and acetylcholinesterase (4EJN). Stigmasterol demonstrated a robust binding affinity for EGFR and acetylcholinesterase among the evaluated chemicals, indicating its potential role in kinase modulation and neuromuscular inhibition of parasites.

Helminthiasis, while instigated by parasitic worms, exhibits pathological manifestations that are predominantly influenced by host biological processes. These processes encompass immune regulation, inflammatory responses, oxidative stress, and mechanisms of tissue repair. In this study, human protein targets were utilized in the network pharmacology analysis to elucidate host signalling pathways that could potentially be influenced by the phytoconstituents of *N. hydrophyllum*. This host-directed approach is commonly utilized in network pharmacology investigations to clarify the molecular mechanisms that contribute to therapeutic effects and to pinpoint potential targets associated with disease progression and host–parasite interactions.

Therefore, this study elucidates the molecular underpinnings of the traditional medicinal significance of *N. hydrophyllum* and underscores its potential as a viable source for the formulation of innovative plant-derived anthelmintic therapies. Additional experimental validation through *in vitro* and *in vivo* studies is essential to assess the efficacy and safety of the identified bioactive compounds.

Acknowledgement

The authors sincerely acknowledge the Central Instrumentation Laboratory, Central University of Punjab, for providing facilities and technical support for the GC–MS analysis conducted in this study.

Conflict of interest

All authors declare no conflict of interest.

References

1 Latif R & Nawaz T, Medicinal plants and human health: a comprehensive review of bioactive compounds, therapeutic effects, and applications. *Phytochem Rev*, 25 (2026) 2299.

2 Khan ZR, Chowdhury NS, Sharmin S & Sohrab MH, Medicinal values of aquatic plant genus Nymphoides grown in Asia: A review. Asian Pacific *J Trop Biomed,* 8 (2018) 113.

3 Konwar A & Shah RK, Medicinal plants for helminth treatment in Assam: Bridging indigenous knowledge with pharmacological research. *Pharmacol Res - Nat Prod*, 10 (2026) 100508.

4 Khairuzzaman M, Hasan MM, Ali MT, Mamun AA, Akter S, Nasrin P, Islam MK, Nahar AU, Sarker DK, Hamdi OAA, Uddin SJ, Seidel V & Shilpi JA, Anthelmintic screening of Bangladeshi medicinal plants and related phytochemicals using *in vitro* and *in silico* methods: An ethnobotanical perspective. *J Ethnopharmacol,* 328 (2024) 118132.

5 Chen CY, Cheng TP, Hwang TL, Hou YS, Salendra L, Ke TY & Cheng YB, Anti-Inflammatory Saponins From an Edible Aquatic Plant Nymphoides hydrophylla. *Phytochem Anal,* 36 (2025) 1710.

6 Kim TY, Park NJ, Jo BG, Lee BS, Keem MJ, Kwon TH, Kim KH, Kim SN & Yang MH, Anti-Wrinkling Effect of 3,4,5-tri-O-caffeoylquinic Acid from the Roots of Nymphoides peltata through MAPK/AP-1, NF-κB, and Nrf2 Signaling in UVB-Irradiated HaCaT Cells. *Antioxidants*, 12 (2023) 1899.

7 Amin A, Tuenter E, Exarchou V, Upadhyay A, Cos P, Maes L, Apers S & Pieters L, Phytochemical and Pharmacological Investigations on Nymphoides indica Leaf Extracts. *Phytother Res*, 30 (2016) 1624.

8 Ko HJ, Huang SH & Ng LT, Chemical Compositions and Antioxidant Activities of a Specialty Aquatic Vegetable Nymphoides hydrophylla in Taiwan. *J Aquatic Food Prod Technol*, 23 (2014) 591.

9 Agyare C, Spiegler V, Sarkodie H, Asase A, Liebau E & Hensel A, An ethnopharmacological survey and *in vitro* confirmation of the ethnopharmacological use of medicinal plants as anthelmintic remedies in the Ashanti region, in the central part of Ghana. *J Ethnopharmacol,* 158 (2014) 255.

10 Abubakar AR & Haque M, Preparation of Medicinal Plants: Basic Extraction and Fractionation Procedures for Experimental Purposes. *J Pharm Bioallied Sci,* 12 (2020) 1.

11 Wallace WE & Moorthy AS, NIST Mass Spectrometry Data Center Standard Reference Libraries and Software Tools: Application to Seized Drug Analysis. *J Forensic Sci,* 68 (2023) 1484.

12 Daina A, Michielin O & Zoete V, SwissADME: a free web tool to evaluate pharmacokinetics, drug-likeness and medicinal chemistry friendliness of small molecules. *Sci Rep*, 7 (2017) 42717.

13 Banerjee P, Kemmler E, Dunkel M & Preissner R, ProTox 3.0: a webserver for the prediction of toxicity of chemicals. *Nucleic Acids Res*, 52 (2024) W513.

14 Daina A, Michielin O & Zoete V, SwissTargetPrediction: updated data and new features for efficient prediction of protein targets of small molecules. *Nucleic Acids Res,* 47 (2019) W357.

15 Stelzer G, Rosen N, Plaschkes I, Zimmerman S, Twik M, Fishilevich S, Stein TI, Nudel R, Lieder I, Mazor Y, Kaplan S, Dahary D, Warshawsky D, Guan-Golan Y, Kohn A, Rappaport N, Safran M & Lancet D, The GeneCards Suite: From Gene Data Mining to Disease Genome Sequence Analyses. *Curr Protoc Bioinformatics*, 54 (2016) 1.30.1-1.30.33.

16 Hu Y, Guo X, Yun Y, Lu L, Huang X & Jia S, DisGeNet: a disease-centric interaction database among diseases and various associated genes. *Database (Oxford)*, (2025) 1.

17 Szklarczyk D, Nastou K, Koutrouli M, Kirsch R, Mehryary F, Hachilif R, Hu D, Peluso ME, Huang Q, Fang T, Doncheva NT, Pyysalo S, Bork P, Jensen LJ & von Mering C, The STRING database in 2025: protein networks with directionality of regulation. *Nucleic Acids Res,* 53 (2025) D730.

18 Shannon P, Markiel A, Ozier O, Baliga NS, Wang JT, Ramage D, Amin N, Schwikowski B & Ideker T,

Cytoscape: A Software Environment for Integrated Models of Biomolecular Interaction Networks. *Genome Res*, 13 (2003) 2498.

19 Ge SX, Jung D & Yao R, ShinyGO: a graphical gene-set enrichment tool for animals and plants. *Bioinformatics*, 36 (2020) 2628.

20 Tang D, Chen M, Huang X, Zhang G, Zeng L, Zhang G, Zeng L, Zhang G, Wu S & Wang Y, SRplot: A free online platform for data visualization and graphing. *PLoS One*, 18 (2023) e0294236.

21 Berman HM, Westbrook J, Feng Z, Gilliland G, Bhat TN, Weissig H, Shindyalov IN & Bourne PE, The Protein Data Bank. *Nucleic Acids Res,* 28 (2000) 235.

22 Kim S, Thiessen PA, Bolton EE, Chen J, Fu G, Gindulyte A, Han L, He J, He S, Shoemaker BA, Wang J, Yu B, Zhang J & Bryant SH, PubChem Substance and Compound databases. *Nucleic Acids Res*, 44 (2016) D1202.

23 O'Boyle NM, Banck M, James CA, Morley C, Vandermeersch T & Hutchison GR, Open Babel: An open chemical toolbox. *J Cheminform*, 3 (2025) 33.